PERGAMON

Carbon 40 (2002) 2063–2083

CARBON

Unpaired π-spin density in defected graphite

O. Ivanciuc, D.J. Klein*, L. Bytautas[1]

Texas A&M University at Galveston, Galveston, TX 77553-1675, USA

Received 18 April 2001; accepted 12 December 2001

Abstract

Simple rules not requiring machine computation are enunciated to predict unpaired π-electron spins in graphitic structures, and these rules are illustrated in application to defected graphites with boundaries (i.e. with edges) or with local vacancy defects. The rules follow from a simple resonance-theoretic argument to give the number and general location of unpaired or nearly unpaired electrons. In addition a band-theoretic scenario for edge- or defect-localized unpaired electrons is outlined. Tight-binding molecular orbital theoretic computations are reported to compare against the resonance-theoretic predictions. The favorability of the comparisons tends to validate our easily applicable generalization of traditional resonance-theoretic organic chemical rationale, now in application to patterns of π electronic behavior for extended graphitic systems with defects.

1. Introduction

The carbon network of graphite and the behavior of the π electrons therein have long been of interest, with theoretical work most commonly focused on bulk properties. The whole area of extended conjugated π network systems is of continuing intense interest, especially with the advent of fullerenes [1,2], of carbon nanotubes [3–5], and of other related possibilities, presumably of much relevance for nanostructural devices—see e.g. [6–11].

On the experimental side, real graphite has boundaries or edges as well as internal defects, and often markedly so, in the sense that most graphite is somewhat impure, consisting of relatively small pieces. Experimentally occurring graphites seem often to be ill-characterized as to the nature of the edges or of the imperfections, and instead often seem to be characterized as to bulk structural characteristics [12–16], magnetic properties [17–19], or chemical properties [20].

Thus theoretical work on the effect of different graphitic boundary structures and defects on the behavior of the π electrons may be especially valuable, and of particular interest would be simple rules correlating molecular structure and the consequent π electronic energy-level patterning, as should sensitively influence magneto–electric properties. Also such structure–property correlations could also be of much use for the characterization of carbon network nanostructures [6–11], which often are closely related to graphite in structure.

Graphite and graphitic edges have historically received some theoretical attention. Within the simple tight-binding (molecular- or band-orbital) framework, quantitative solutions [21–23] for the π electron bands of extended graphitic systems go back a half century, and now there are hundreds of more recent band-theoretic articles. But especially for conjugated π networks Pauling and Wheland [24] had advocated the so-called resonating valence bond (VB) view as providing much chemical insight, so that this approach has become much used for such conjugated hydrocarbon molecules, at least so long as the molecules are not extended structures, such as graphite. Indeed Wheland wrote an influential monograph [25] concerning such ‘benzenoid’ molecules, and Pauling generalized his ideas to cover the whole of chemistry in his masterwork [26] on The Nature of the Chemical Bond. Furthermore Pauling’s view encompassed the possibility of extended structures, and he wrote a qualitative discussion [27] on bulk graphite, and related undefected structures. But quantitative semiempirical work within a resonating valence bond (VB) framework perhaps only starts with Refs. [28,29] in 1984. And since then there has been much more work on semiempirical VB-based computations, though much of it has been directed to treating fullerenes, or

*Corresponding author.

E-mail address: kleind@tamug.tamu.edu (D.J. Klein).

[1]On leave of absence from Institute of Theoretical Physics and Astronomy, Vilnius, Lithuania.

0008-6223/02/$ – see front matter
PII: S0008-6223(02)00065-9

conjugated polymers, or also high-temperature superconductors—a broad yet brief overview of all this being found in [30], while an intensive discussion focusing on this last aspect (concerning high-temperature superconduction) may be found in several reviews in the physics literature [31–34]. A simplified sort of resonance-theoretic treatment simply enumerates Kekule structures (taken as nearest-neighbor spin–pairing patterns, with the spin pairings maximized), this approach being suggested by Pauling and Wheland [24–26], and now extensively developed, as reviewed, e.g. by Cyvin and Gutman [35] for many polyhex fragments of specific shapes cut from a graphite lattice.

As to edges (or surfaces) on semi-infinite structures, the most common theoretical approach to general structures has been via (quantitative) semiempirical molecular-orbital (MO) theory, so that common monographs (as [36,37]) addressing such matters discuss this approach exclusively. And actually starting about a half century ago such MO- or band-theoretic results concerning graphitic edges were reported [21,38]. Qualitative resonance-theoretic discussion of graphitic edges seems to start in 1985, with [39], and another near-simultaneous independent discussion is found in the works of Stein and Brown [40–42], though there the manner of application of the resonance-theoretic ideas might be taken to be unsuccessful in giving results seemingly interpretable as at variance with MO-theoretic results. Their MO-theoretic results did however indicate a novel possibility for nonbonding edge-localized MOs for some edge structures, while not so for others.

From a general empirical view, the relevance of edges in understanding several characteristics of graphite (especially as regards activation and passivation) has often been recognized; e.g. this is emphasized by Urry [20] in 1987. More recently there have been a number of tight-binding band-theoretic studies seeking [43–49] to characterize the effects of different types of edges on the π-electronic structure of graphite. Particularly for some types of edges, the theoretical results predict unpaired-spin density localized near the edges, with consequent effects—say, concerning reactivity and paramagnetism, and perhaps also these edge-localized electrons may be particularly favorable for electrical conduction.

A further topic of study concerns local defects in graphite, though there seems to be but a couple references [50,51] back in the 1960s, and more recently a few more [49,52–56]. The MO-based references [50–55] concern only a single-site vacancy defect in graphite, while [56] also considers a two-site defect, though clearly there are many other possibilities. As discussed by Coulson et al. [50] there is good reason to believe that some such types of defects are ubiquitous in graphite, under suitable circumstances.

Here the use of simple resonance-theoretic rules to treat defected graphites is pursued.

Numerous illustrations are provided, all for a diverse selection of defected graphitic structures, including a variety of (single- or multisite) local vacancy defects and separated pairs of local defects as well as linear defect of different sorts of edges (cut along different directions of the graphite lattice). Further MO-based numerical tests of the predictions are reported. Section 2 describes the general theory, while Section 3 reviews briefly its application to benzenoid molecules, for which reliable results are otherwise known. Section 4 goes on to consider the case of edges in semi-infinite graphite, while Section 5 considers the case of local vacancy defects, and finally Section 6 considers the case with two separated such local defects. Sections 7–9 describe MO-based tests of the predictions for edges, for local vacancy defects, and for pairs of such defects. Sections 10 and 11 go on to briefly mention the circumstance with other related local defect structures and substitutional defects. Finally Section 11 offers a discussion of the resultant progress in understanding the structure and properties of defected graphites.

The simple resonance-theoretic rules have already been enunciated [48,49,57] and extend traditional organic chemical presentations in making fundamental use of the fact that graphitic networks treated may be partitioned into two sets, such that any site of one set has all its near neighbors in the other set. In the solid-state literature such sets are often described as those of A and B sublattices, and in the MO organic chemical literature the sites of the two sets are often called starred and unstarred. For instance, for 1,3,5-trimethylenebenzene one has the starring and unstarring as indicated in Fig. 1. The relevance of such partitioning may be viewed as implicit in some early resonating valence-bond developments [24,58,59], but emphasis on its special relevance seems to be first found in MO work by Coulson and Rushbrooke [60], who established a neat theorem concerning the Hückel MO spectrum for molecules which could be so partitioned into starred and unstarred sets. Such MO-based ideas are now commonly found in organic chemistry texts and the conjugated systems with starred and unstarred subsets are commonly called alternant, and in the mathematical theory of graphs they are called bipartite.

Notably graphite as well as a diversity of different defected graphites are so alternant, and the simple reso-

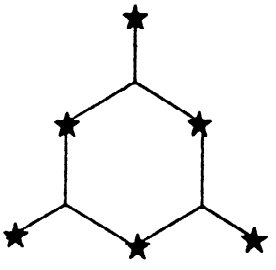

Fig. 1. Starring and unstarring for 1,3,5-trimethylenebenzene.

nance theory we have developed presumably applies to these structures, whether they involve edges on semi-infinite graphite or various sorts of local defects within graphite.

Throughout the present paper the π network is considered only in so far as providing a frame in which the π electrons are to move. Of course with edges or internal vacancy defects there are σ electrons at the boundary to the defect, so that most favorably they should be bonded to some atoms or groups of low valency, such as H atoms. If the bonds are instead allowed to 'dangle' there could conceivably be some sort of reconstruction of the edge to a strained structure. Here it is imagined that no such reconstruction occurs, so that the structure of the network up to the edge or up to the local region of a vacancy region is just a subsection of an infinite graphite sheet. That is, the structures presently presumed are to be just simple little-distorted subsections of the honeycomb lattice. If the σ electrons from the carbons at the edges were bonded to –OH or =O groups (instead of H-atoms), then there would in a more complete description be additional π electrons (from the O atoms) to take into account.

Though such circumstances might be treated, we proceed in the present work presuming solely C atom π electrons.

2. Qualitative resonance theory for molecular or extended graphitic structures

Conventional qualitative resonance theory [25,26] is based upon the consideration of sets of different classical chemical-bonding patterns consistent with the given structure. In resonance theory each carbon of a neutral conjugated network is viewed to have one π electron, and the chemical-bonding patterns are actually thought of as identifying singlet spin pairings between such π electrons. As a first important point it is presumed that all ground-state spin pairings may be taken to be between electrons on different types (★ and ○) of sites. For overall spin singlet states this was long ago noted by Rumer [58] and incorporated [59] in the development of a systematic VB basis for overall spin singlets. Pauling [61] extended this idea to the spin doublet manifold, while other more recent works have extended this Rumer-type basis selection to arbitrary spin multiplicities—see e.g. Simonetti et al. [62] or Pauncz's review [63]. Generally neighbor spin pairing leads (in the Pauling–Wheland VB model) to energy lowering, and of course this is between sites of different (★ and ○) types, and Rumer showed that if one locally modifies such a neighbor-paired pattern so as to pair up (two pairs) of sites of the same type, then this turns out to be a linear combination of states solely with different types of sites spin-paired (although they may not turn out to be nearest neighbors). We imagine that spin-pairing (for the ground state of alternant systems) has spin-pairing solely between different-type (★ and ○) sites. This is also consistent with a theorem (for ground-state spins of a Heisenberg model) as announced by Lieb and Mattis [64] (see also [65]).

Granted the criterion of spin-pairing always between different types of sites (★ and ○), the key points of Pauling's resonance theory may be indicated. Basically the greater the number of low-energy VB spin-pairing patterns the greater the stabilization (because of quantum-mechanical 'configuration interaction' amongst them). And of course an individual VB bonding pattern is lower in energy the greater the number of neighbor singlet spin-paired bonds there are.

Thus there are two tendencies competing to maximize overall energetic stability

(loc) maximization of the number of more locally paired sites;
(res) maximization of the number of like-energy resonance structures

and the first locality tendency is often somewhat more important. A traditional approach, most successful for small molecules, simply enumerates [35] nearest neighbor spin-pairing patterns, for which there is a maximum number of spin pairings—but this presumes the complete dominance of the first rule (loc) over the second (res). More generally, the resonance condition can become more important when the cost in numbers of pairing patterns is much greater than the number of neighbor pairs sacrificed in such patterns. Thus for instance, since the edge is such a small fraction of the bulk (if the graphitic fragments are large), one might allow non-neighbor paired sites confined to the region of the edges, if this circumstance notably enhances the number of VB spin-pairing patterns. That is, in resonance stabilization for a large number N of atoms, the bulk might overcome the loss of the relatively few $\sim N^{1/2}$ unpaired π electrons near the edge. (At least for 'ordinary' shaped fragments, the boundary should have $\sim N^{1/2}$ atoms.)

Thus the argument devolves to the consideration of classes of VB bonding patterns with satisfaction of the first rule above indicating that any non-neighbor-paired sites should be confined to the edge region. Then in consequence of the second rule, such classes having the greatest numbers of members are sought. Ordinarily one views the problem in principle to devolve to the generation of what turns out to be vast numbers of valence structures, and thence to be only modestly simplified in looking just to enumerate the structures. But in fact the characterization of the class of most numerous VB pairing patterns is somewhat intuitively clear: resonance should be greatest when the pairing patterns have bonds delocalized as much as possible subject to being between near neighbors (for the most part). That is, one might anticipate that in the bulk region the probability of a double bond along any one of

the three directions away from a site to its nearest neighbors is equally likely. This probability though is essentially a bond order as is often defined [66,67] in treating benzenoid molecules: the Pauling bond order for a given bond of a conjugated hydrocarbon is just the fraction of the neighbor-paired patterns (often called Kekule structures) for which the given bond is double. For benzene, naphthalene and trimethylenemethyl the Pauling bond orders are as indicated in Fig. 2. For large graphitic fragments the preferred classes of VB pairing patterns should be those such that the π-bond orders are very close to 1/3 in the bulk of the fragment.

But now there are notable consequences granted that the π-bond orders are close to 1/3 in the bulk and that any deficit of the sum of the bond orders at any site of lower degree (as near a fragment edge) represents non-neighbor paired electron density. This deficit might be termed a residual-free valence.

A further refinement concerns the range of any pairing between non-neighbor sites. If the distance between two non-neighbor sites is smaller, then such a pattern being more similar to a preferred neighbor-pairing pattern is more stabilizing than a pattern with free valences which are necessarily very distant. That is, the free valences on the ★ and ○ (or A and B) sites might be identified with + and − signed spin densities with spin pairing only between opposite signed spin densities, with the strength of the pairing diminishing with separation. The overall argument may be expressed as a simple set of rules:

(a) Assign 0-order π-bond orders of 1/3 to each edge issuing from a site of degree 3.
(b) Assign the remaining π-bond orders to be as large as possible subject to the constraint that the sum of the π-bond orders into no site exceeds 1.
(c) Calculate 0-order free valences v_i at each site i as the deficit from 1 of the sum of the π-bond orders p_e incident at that site (i.e. $v_i = 1 - \Sigma_{e-i}\ p_e$).

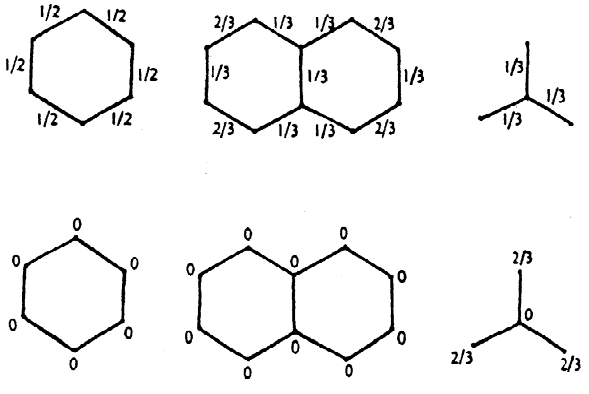

Fig. 2. Pauling bond orders for benzene, naphthalene and trimethylenemethyl.

(d) The unpaired spin density at an edge is the difference between the net free valence of ★ and ○ sites nearby on an edge.

Again a refinement of the last two rules would take more explicit account of pairing between next-next-nearest neighbors (or perhaps even a little more distant), thereby identifying generally more accurately the unpaired spin density and its location.

3. Benzenoid molecules

The resonance theory of the preceding section leads to a clean prediction for the number of unpaired electrons in the ground state of a benzenoid. Let $n_{j\star}$ denote the number of starred carbons each bonded to j other carbons, and $n_{j\circ}$ denote the number of unstarred carbons each bonded to j other carbons. Then the net 0-order free valence at starred sites is $(2n_{1\star} + n_{2\star})/3$ and at unstarred sites is $(2n_{1\circ} + n_{2\circ})/3$. But since in higher orders the electrons of these various free valences from one set may be spin-paired with those from the other until electrons of one type or the other becomes depleted, it must be that ultimately (as in ∞-order) the number of unpaired electrons is

$$u = |2n_{1\star} + n_{2\star} - 2n_{1\circ} - n_{2\circ}|/3 \quad (1)$$

Evidently one may very readily make a variety of predictions. An alternative expression may be made if one notes that the number of carbon–carbon σ bonds is counted both by $n_{1\star} + 2n_{2\star} + 3n_{3\star}$ and by $n_{1\circ} + 2n_{2\circ} + 3n_{3\circ}$. Then the first of these is added to the term $2n_{1\star} + n_{2\star}$ in (1) and the second of these to the term $2n_{1\circ} + n_{2\circ}$ (as is subtracted in (1)), so as to recast Eq. (1) to

$$u = |n_\star - n_\circ| \quad (2)$$

with $n_\star$ and $n_\circ$ simply the respective net numbers of starred (★) and unstarred (○) carbon sites. This is a result known [63,64] to be true by theorem for the full VB model with near-neighbor exchange couplings (which is also called the antiferromagnetically signed Heisenberg model, with site spins of 1/2). In fact it turns out to be true by theorem [68] for the half-filled Hubbard model, and yet further, when tested by brute force computations on a full Pariser–Parr–Pople model, the result remains [69] true for all chemical alternant structures of nine or fewer sites. There is a large degree of agreement of this prediction with even more accurate ab initio computations and experiment, as briefly reviewed in [57].

Moreover, the present resonance theory makes predictions as to the location of unpaired spin density and the possible occurrence of low-lying states of higher spin multiplicity (if the pairing patterns necessarily entail pairings between very distant sites). In particular, the predictions as to locations of spin density turn out (for the

present molecular case) to be consistent with theorems [65,70,71] for the Heisenberg model concerning signs of spin densities and signs of spin-coupling expectations.

Therefore for finite benzenoids the resonance theory seems to be quite reasonable, and easy to apply. For MO-theoretic approaches to attain agreement they generally need to be extended beyond the use of Hund's rule as applied to the Hückel model. This was developed in a series of papers (e.g. [72–75]) by Borden and Davidson, with some review in [76] as well as [57].

4. Resonance-theoretic predictions for graphitic edges

The resonance-theoretic rules seem fairly readily applicable, and for translationally symmetric edges they lead to a simple purely structural characterization. Rule (d) uses the phrase 'nearby' which for the case of translational symmetry can be given a quite precise formal meaning, in terms of sites within the same unit cell of edge. Further in looking at the net spin density the precise locality of the unpaired spins does not matter, so that one might use just a 0-order picture with a bond-order of 1/3 (initially) assigned to every bond and the corresponding 0-order free valences are 0, 1/3, 2/3, or 1 for sites of respective degrees $v = 3$, 2, 1, or 0, though of course we still need to pay attention to further (more distant) pairing between opposite types of sites.

There results a simple purely structural rule for the number of unpaired electrons per unit cell of edge

$$\#_u = |2\#_{\star 1} + \#_{\star 2} - 2\#_{\circ 1} - \#_{\circ 2}|/3 \qquad (3)$$

where $\#_{\star v}$ and $\#_{\circ v}$ are the numbers of degree-v starred and unstarred sites per unit cell of edge.

This simple result may be applied in a number of cases. For the two kinds of regular (i.e. translationally symmetric) edges appearing in Fig. 3 there is pairing between either nearest neighbors or next-next-nearest neighbors, so that these edges are not so reactive. But for the different types of regular edges in Fig. 4 there is pairing possible only to some distant sites, say on an opposite edge, so that these edges may be expected to be reactive, and exhibit essentially unpaired spin density localized along the edges of the fragment—that is, these edges are polyradicaloid. Moreover, these ideas apply to characterize many other types of edges. A more comprehensive listing of Fig. 5 identifies just a unit cell of edge, and indicates the low-order spin pairings possible.

A further general result depends on the translational symmetry characteristic of the edge.

The unit cells are conveniently labelled by the primitive translations along the edge direction, such a label being a two digit code (x,y) with x identifying the number of hexagon-center to neighbor hexagon-center steps along one direction imagined to be from left to right and y identifying the number of similar steps along a second direction rotated 60° counterclockwise. It is a matter of convention to choose

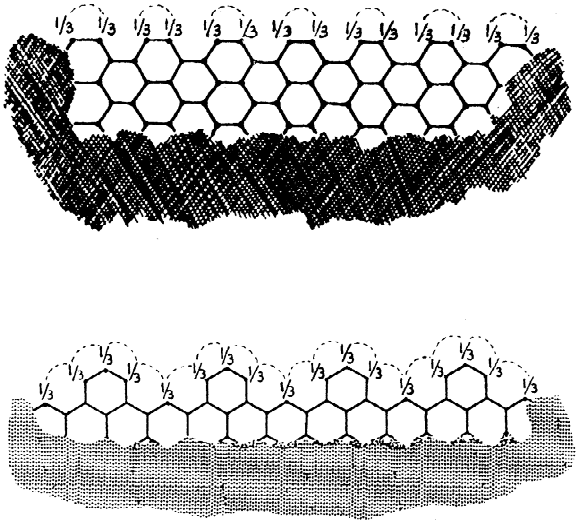

Fig. 3. Two regular (i.e. translationally symmetric) edges for which there is a low-order spin-pairing between either nearest neighbors or next-next-nearest neighbors, so that these edges are predicted to give rise to no edge-localized unpaired electrons. The non-zero 0-order free valences are indicated, with interconnecting dashed lines to indicate spin-pairing beyond 1st-order.

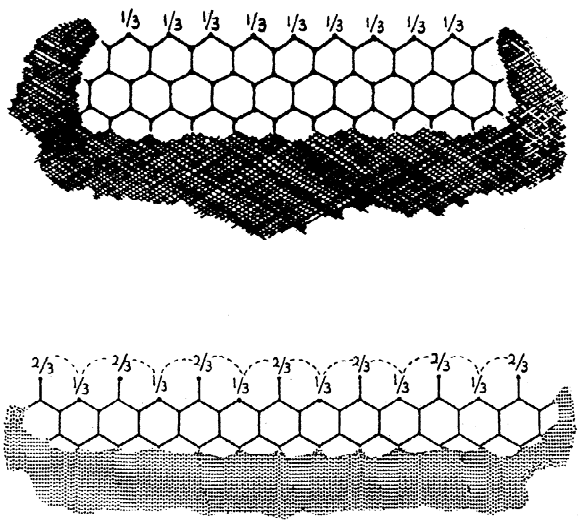

Fig. 4. Two regular (i.e. translationally symmetric) edges for which there is no low-order spin-pairing to deplete all the free-valence near the edges, whence it is predicted that there are edge-localized unpaired electrons. Note that for the second of the two edges there is some (incomplete) spin-pairing beyond 1st-order. Here each dashed line may be viewed to indicate a higher-order pairing for 1/6 of an electron per interconnected site.

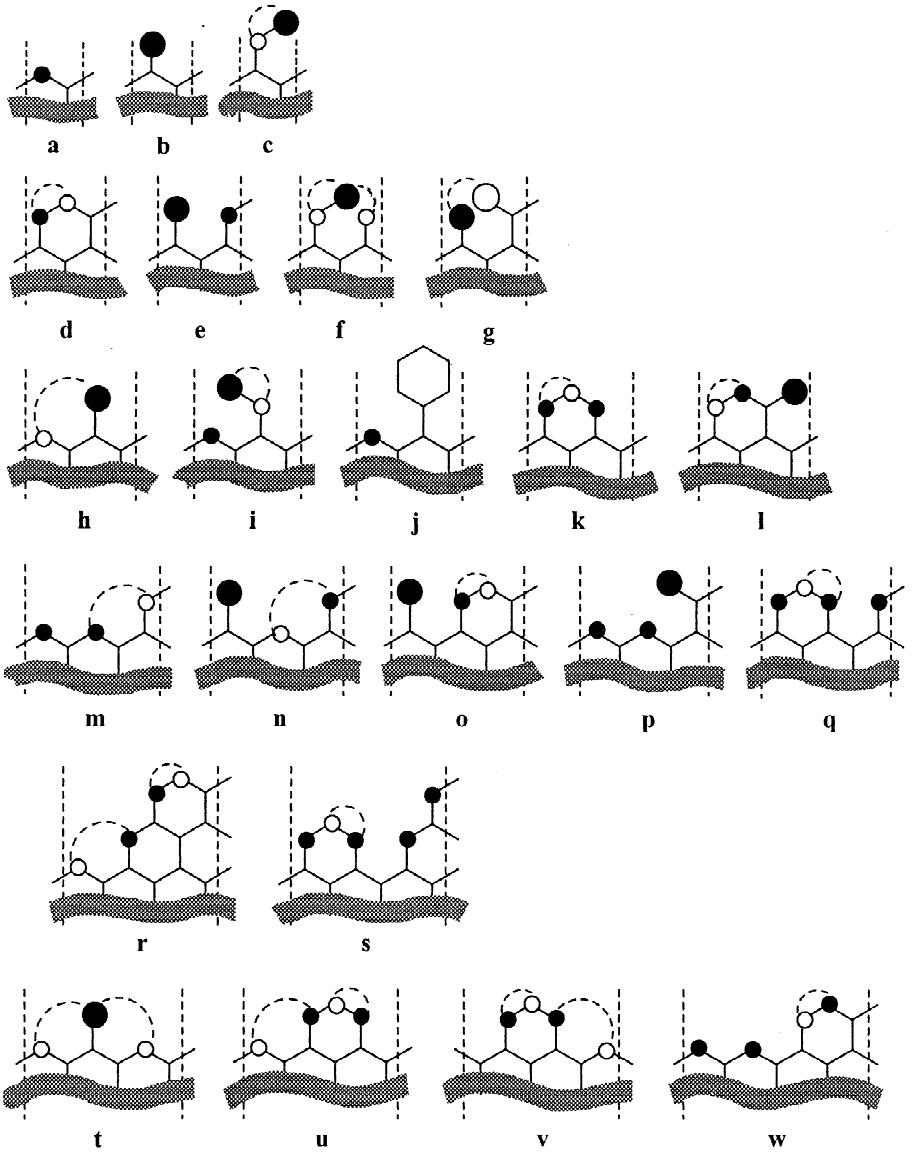

Fig. 5. Unit-cell portions of a variety of possible graphitic edges. Here the vertical dashed lines indicate the boundaries of the unit cells, and zero-order free valences (of 1/3 or 2/3) at a site are indicated by (small or large) circles at that site, with the circle being solid or hollow as the site is starred or unstarred. Additional pairing beyond zero-order is indicated by curved dotted lines, each dotted line indicating the pairing of 1/6 of an electron (at each end of the line).

$$0 < x \geq y \geq 0 \qquad (4)$$

The edge symmetries for the edges of Fig. 3 are, respectively $(x,y) = (1,1)$ and $(3,0)$, while those of Fig. 4 are $(x,y) = (1,0)$ and $(2,0)$. Then we have a general result which allows one to exclude many symmetry classes of edges from ever being nonradical, namely:

Symmetry-integrality theorem—within the simple resonance-theoretic picture as applied to translationally symmetric edges of symmetry class (x,y), the number $\#_u$ of unpaired electrons per unit cell is an integer if and only if f $x - y$ is an integer multiple of 3.

A proof has been previously given [48]. But in particular this implies that the only edges which might have no edge-localized unpaired electrons are those for which $x - y$ is an integer multiple of 3 (counting 0 as such a multiple). In particular this theorem accounts for the unpaired electrons for the cases of Fig. 4.

For the polyradicaloid case the unpaired spin densities are not necessarily so severely localized as one might

surmise from the simplified low-order approximation considered here. That is, one can imagine the free valences locally moved around to other nearby atoms, as done in Fig. 6. But the overall free valence on all sites is conserved (as is more or less empirically evident, but which was proved in [48]). Rearrangement of the bond orders allows the free valences to be more smeared out, but still gives rise to the same net numbers of unpaired electrons near the edge. Thus even without explicit construction of Kekule structures, predictions are readily reached as to the net extent of unpaired electrons showing up on a given type of graphitic edge, and some indication is obtained of where the unpaired spins show up.

Of course sites with higher residual free valences should be more reactive. That is, if a site forms with higher free valence values, then one can anticipate that the site is reactive, preferably forming (say, through addition reactions) new local structures which exhibit less free valence. Thence there are implications as to the types of stabilized edges as could appear on large graphite fragments. Also unpaired electrons at the edges should enhance a material's paramagnetism, which is in fact observed for some graphites, with some graphitic materials showing [17–19] exceptional paramagnetism, perhaps because of unusual edge structures. Further there should be implications for regular conjugated hydrocarbon polymer strips, several simpler types of which have received much experimental treatment over the last couple of decades—notably polyacetylene and poly-*p*-phenylene [77,78]. Indeed similar ideas apply to correlating locally unpaired spin densities at the ends of polymer strips with the type of strip structure and the various end structures, but this we do not pursue here, it having already been done via the present approach [49] or via a more traditional resonating VB approach [79,80]. It is emphasized that the resonance-theoretic approach may be elaborated with more quantitative overtones, though that is not addressed here.

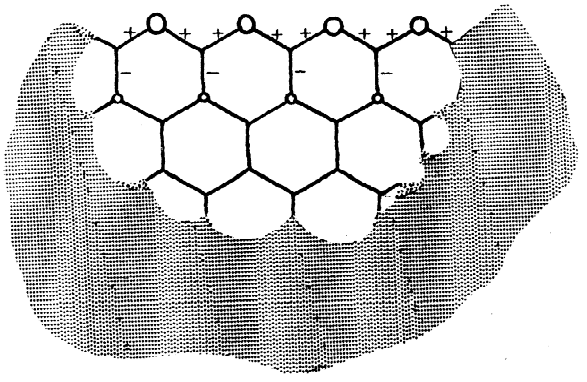

Fig. 6. Modified assignment of bond orders for the same boundaries as in the first example of Fig. 4. Here the bonds marked with a + are to have a bond order of 7/18 (i.e. slightly enhanced from the 0-order value of 1/3), those marked with a − are to have bond order 2/9 (i.e. slightly depleted slightly from the 0-order value of 1/3), and those which are unmarked are all to have the 0-order value of 1/3. The consequent free valences are 2/9 at the peripheral sites with bigger circles and 1/9 at the more interior sites marked with little circles. Note that the same overall amount of residual free valence remains and that it remains on the same type of sites—that is, the net number of unpaired electrons remains the same (on the same type of sites).

5. Resonance theoretic predictions for vacancy defects

The question of the effect of local vacancy defect structures in otherwise perfect graphite may also be addressed via resonance theory [49]. One may delete one or more contiguous carbon atoms from the graphite lattice, thereby giving what we term an antimolecule corresponding to the molecule consisting of the internally still connected set of deleted atoms. Thus with deletion of a single C atom we obtain 'antimethyl', and with deletion of two adjacent atoms we obtain 'antiethylene', and with the deletion of three consecutive atoms we obtain 'antiallyl'. The resonance-theoretic predictions are relatively straightforward to make, as illustrated in Fig. 7. In fact one may perceive a general pattern. Note the perfect graphite has a local balance of starred and unstarred sites, and note that in the formation of an antimolecule $\mathcal{Я}$ by deletion of the π network corresponding to a molecule R, the unbalance of starred and unstarred sites in the region of the antimolecule must be the same (except for sign) as the unbalance in the corresponding molecule R. That is, for methyl, ethylene, and allyl one has an unbalance of 1, 0, and 1, so that this should also be the regional unbalance in site types for antimethyl, antiethylene, and antiallyl, respectively, and this then leads to this consequent number of unpaired electrons, to be localized in the region of the corresponding defect (i.e. of the corresponding antimolecule $\mathcal{Я}$).

Thus for a general molecule R with numbers $\#_\star$ and $\#_\circ$ of starred and unstarred sites, our mean-field resonance theory predicts (as discussed in Section 3) a number $|\#_\star - \#_\circ|$ of unpaired sites, and the present argument leads to the prediction that the number of defect-localized unpaired electrons for the corresponding antimolecule $\mathcal{Я}$ in graphite is

$$\{\#\ \mathcal{Я}\text{-localized unpaired e}\} = \{|\#_\star - \#_\circ| \text{ for R}\} \qquad (5)$$

Indeed this result of matching of properties (in particular of net spin densities) for the molecule and antimolecule, in part justifies our choice of nomenclature of 'antimolecules' for our vacancy defects.

6. Resonance-theoretic predictions for pairs of vacancy defects

The argument of the preceding section in fact readily extends to pairs of vacancy defects; or alternatively stated,

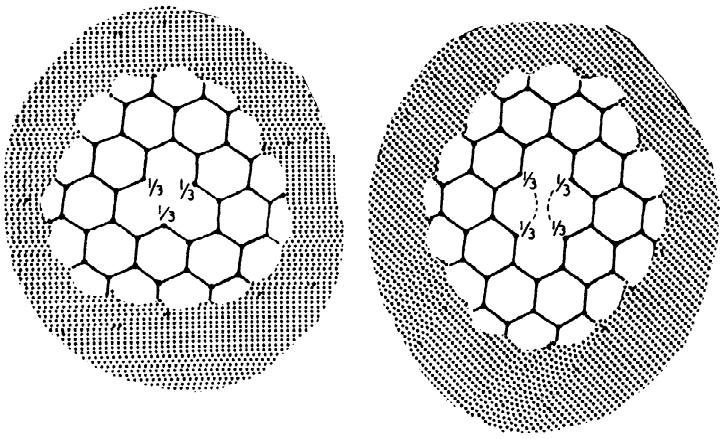

Fig. 7. Antimethyl and antiethylene vacancy defects in graphite, showing 0-order resonance bond orders, and any additional spin-pairing (beyond 0-order) is indicated with dashed lines.

it readily extends to characterize the interaction between pairs of antimolecules. Such a pair of antimolecules Я and Я′ at a given not too large separation still occur in a local region of the ambient graphitic network, and then can be viewed as a bimolecular antisuper-molecule ЯЯ′. Thence the number of defect localized non-bonding orbitals around ЯЯ′ should still be $|\#_{\star} - \#_{\circ}|$ where now $\#_{\star}$ and $\#_{\circ}$ are the net numbers of starred and unstarred sites in R and R′, i.e. $\#_{\star}(RR') = \#_{\star}(R) + \#_{\star}(R')$ and $\#_{\circ}(RR') = \#_{\circ}(R) + \#_{\circ}(R')$. But it is emphasized that the relative dispositions of the two antimolecules with respect to one another is very crucial, since moving just one of the two antimolecules by just one bond length in graphite results in the interchange of starred and unstarred atoms in the moved molecule. That is the counts $\#_{\star}(R')$ and $\#_{\circ}(R')$ are not intrinsic to R′ but depend on the location of R′ relative to R. For instance, we may consider the simple case when the two antimolecules are both methyls, and they may for instance be located in the same hexagonal ring of otherwise perfect graphite, whence there are three distinguishable locations: at 1,2-(or *ortho*-) positions, at 1,3-(or *meta*-) positions, or at 1,4-(or *para*-) positions of the ring; see e.g. Fig. 8. Thence in these three cases we find respective star–unstar imbalances of 0, 2 and 0, and consequent numbers of unpaired electrons of 0, 2 and 0.

Of course the two antimethyls need not be in the same ring, but still we very easily identify the number of unpaired electrons (always as 0 or 2). Clearly this resonance-theoretic argument also readily extends to other pairs of antimolecules (other than two antimethyls).

7. Molecular orbital theoretic scenario and results for edges

In materials science and solid-state physics quantitative band-theoretic arguments and computations are more conventionally made than are resonance theoretic arguments and computations. There are different manners of establishing band-theoretic results, but in treating edge localization effects the most common approach so far explored attempts to treat each different translationally symmetric edge as a separate individual computation. But now for a number of different such edges so investigated

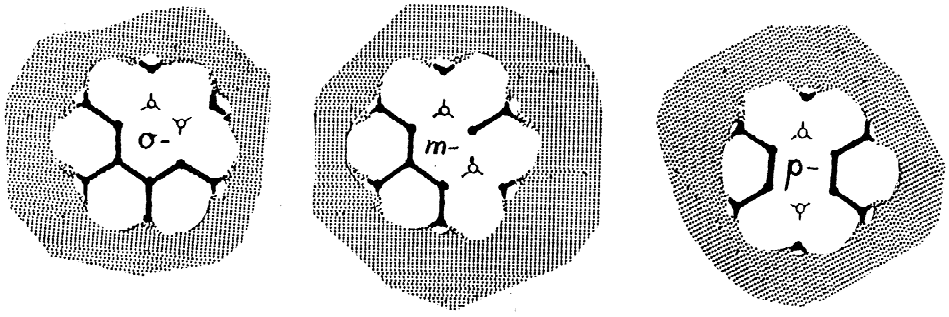

Fig. 8. Three arrangements (*o*-, *m*- and *p*-) of two antimethyls within one hexagonal ring. Each vacancy is marked by a small open circle (to aid in perceiving the corresponding unvacated ring).

[38,43–48], along with some further work here, a general scenario of behavior emerges.

This general band-theoretic scenario is nicely described and implemented in terms of Hartree–Fock (HF) computations on wide strips with two edges but well separated from one another, so that there would be little 'communication' between opposite edges. In such a case with (wide) strips there would be just a finite number of sites per unit cell, thereby facilitating ordinary band-theoretic computations. Basically finite-width strips (with finite unit cells) are labelled by a one-dimensional wave-vector k (corresponding to the translational symmetry along the polymer strip), and one may obtain a band plot of orbital energy vs. k, for the Brillouin zone with $-\pi \leq k \leq \pi$. The molecular orbitals computed within such a picture are smeared out along the length of the polymer strip but usually also across the strip. Still occasionally there are portions of some bands that are exceptional: these edge-localized band orbitals though smeared out along the length of the polymer fall off overall exponentially in amplitude with distance from the edges. Moreover, in many cases such exceptional edge-localized orbitals are very near to the Fermi energy ϵ_F—indeed with orbital energies ϵ approaching exponentially near ϵ_F as the strip width w increases. Then these edge-localized orbitals occur for a portion of a band remaining very flat for the range of k values over which edge-localization occurs. Such a case where edge localization occurs involves the first (acenic) edge of Fig. 4. For this case within the nearest-neighbor tight-binding (Hückel theoretic) approximation, the orbital energies are arranged as indicated in Fig. 9, where the bulk of the bands for any width w are confined to the shaded regions, which are symmetric about the Fermi energy $\epsilon_F = 0$. Indeed there is but a portion of a single bonding band (and a single corresponding antibonding band) which penetrates outside of this shaded region, and this exceptional band is that of the exceptional (edge-localized) orbitals. In Fig. 9 the exceptional band portion is shown for the case of widths $w = 1$, $w = 2$, $w = 3$, and $w = 4$ in the 1st, 2nd, 3rd, and 4th quadrants of the ϵ vs. k plot of the figure. There one sees that this exceptional band portion tends to close-in on the nonbonding $\epsilon_F = 0$ Fermi level in the region where $2\pi/3 < |k| < \pi$ ever more closely as the strip width w increases. The exceptional antibonding orbitals give much the same densities as the bonding orbitals, since these bonding and antibonding orbitals differ in amplitudes only in being symmetric or antisymmetric across the strip, whence the node for the antisymmetric case occurs in the region where even for the symmetric orbital the amplitude is very small (in magnitude). Now any of the nearly degenerate exceptional bonding and antibonding near-degenerate band orbitals (if combined to exhibit localization near just one edge) may be singly occupied with orbitals of different spins for different edges to yield an unrestricted Hartree–Fock (uHF) wave function which may be argued to be of lower energy than the restricted Hartree–Fock

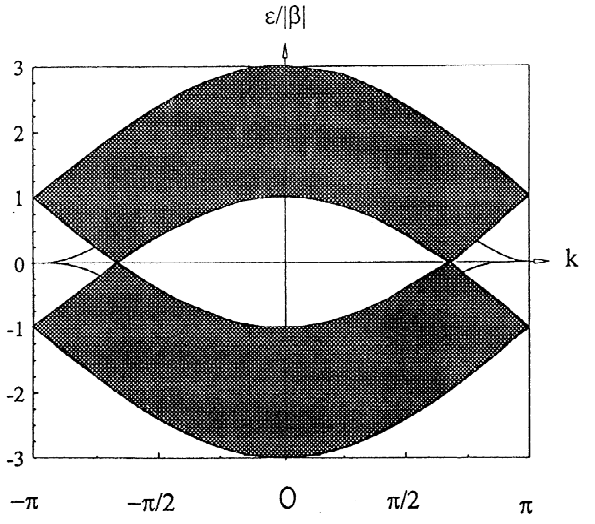

Fig. 9. Overall pattern of band structure for arbitrary width strips with acenic (zig-zag) edges. The bulk bands occupy the shaded region; and the exceptional edge-localized bands penetrate into the regions $-\pi \leq k < -2\pi/3$ and $2\pi/3 < k \leq \pi$, with the displayed bands being for the strips of widths $w = 1$, 2, 3 and 4, respectively appearing in the 1st, 2nd, 3rd, and 4th quadrants of the Brillouin zone.

(rHF) solution. That is, for such exceptional orbitals (of wave-vector k) the cost of the uHF wave-function to the orbital energy is proportional to the corresponding band gap Δ_k which comes ever closer to 0 for ever wider strips when dealing with the noted exceptional edge-localized orbitals; on the other hand, electron-repulsion energy (say proportional to the Hubbard parameter U) is in such cases saved since the uHF orbitals on opposing edges are well separated with differential overlap between orbitals on opposite edges decreasing exponentially fast as w increases. Thus any such exceptional band orbitals give rise (in the uHF approximation for a Hubbard-PPP-type model) to unpaired spin density near the edges. For such systems the restricted HF solutions (for uniform bond length) PPP models are equivalent to the solution of the simple Hückel model, and the ensuant occurrence of certain unrestricted HF solutions can be readily recognized. Notable in this regard is that for alternant systems (as we have) there is [60] a (fairly well-known) 'pairing' symmetry in the eigenvalue spectrum about the nonbonding energy here taken as 0. This symmetry is that for every eigenvalue ϵ there is a corresponding eigenvalue $-\epsilon$. So if there are Hückel molecular orbitals (MOs) which are only very weakly bonding (i.e. MOs with very small magnitude negative ϵ), then there are corresponding very weakly antibonding MOs. Then as a consequence the edge-localized orbitals come in bonding–antibonding pairs which if they correspond to the pairs that are symmetric–antisymmetric across the strip, then they must be nonbonding

(since symmetric–antisymmetric edge-localized pairs must be of very similar energy). Whether a uHF instability occurs of course depends on just exactly how small ϵ is in magnitude (as well as on some details of the exchange interaction for the indicated orbitals). But as it turns out [19,26] for suitable strips of width w the portion of a considered band such as to be especially near the Fermi energy typically exhibit (direct k-dependent) band gaps Δ which scale with width w as $e^{-a/w}$, so that for the limit of wide strips it is assured that this Δ becomes small enough in magnitude for the uHF instability to occur. Moreover, these edge-localized incipiently singly occupied MOs are generally easy to recognize just from an energy-band diagram, because they must occur in a region of this diagram different than the MOs of bulk edgeless graphite which has [21–23] a 0 density of MO levels at the nonbonding energy. That is, if there are a substantial number of edge-localized incipiently singly-occupied MOs (associating to unpaired electrons), then in a standard MO band diagram they should occur as portions of otherwise absent bands very near to $\epsilon = 0$.

With this scenario and its manner of recognition in hand, one may next look to see if it is operative for structures in consonance with the resonance-theoretic predictions. Several Hückel theoretic band diagrams for strips (of widths all taken $w \geq 20$) are shown in Figs. 10 and 11. These plots are for discrete sets of (~25) wave vectors k between 0 and π (it being understood that for k between $-\pi$ and 0 the result is just the same as already shown with a reflection in a vertical plane at $k = 0$). In all these cases the bulk of the bands all fall into a shaded region (shaded because of the density of MO energy points) corresponding to what occurs with bulk (edgeless) graphite. In the cases of Fig. 10 there are bands that penetrate out of the shaded region and hug to a portion of the nonbonding k axis of $\epsilon = 0$, it being these exceptional MOs which must be the edge-localized nonbonding ones. If the portion of such an $\epsilon = 0$-hugging band covers a fraction f of the Brillouin zone, then this corresponds to f unpaired electrons per unit cell. The cases of Fig. 11 are expected from resonance theory to have no edge-localized unpaired electrons, and in this figure we see no nonbonding band penetrating out of the shaded region of bands, so that the band theory also gives no edge-localized unpaired electrons. As a test of the edge-localization features imagined to be associated with the exceptional nonbonding bands of Fig. 10(b), a plot is made in Fig. 12 of the logarithms of the mean densities of several such MOs as a function of their distance from the edge of Fig. 5(j). For such orbitals the density is seen to fall exponentially with distance n from the (nearest) edge, though the exponential fall-off rate is seen to be different for different k values. The edge localization is seen to be

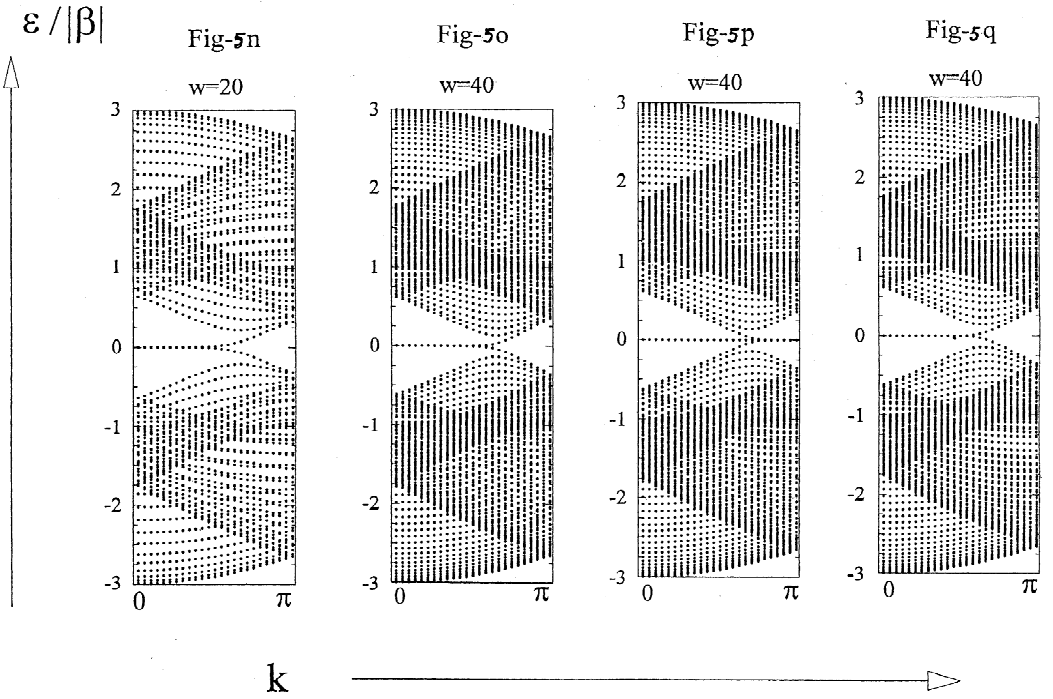

Fig. 10. Band eigenspectra (in units of $|\beta|$) displayed at a selection of 25 different k values uniformly spaced from $k = 0$ to $k = \pi$, for four width w strips each with different edge structures of a type which give rise to nonbonding unpaired electrons, as are associated with the portions of bands which hug the k axis. The four edge structures are (in order): edges as in Fig. 5(n) with $w = 20$; as in Fig. 5(o) with $w = 40$; as in Fig. 5(p) with $w = 40$; and as in Fig. 5(q) with $w = 40$.

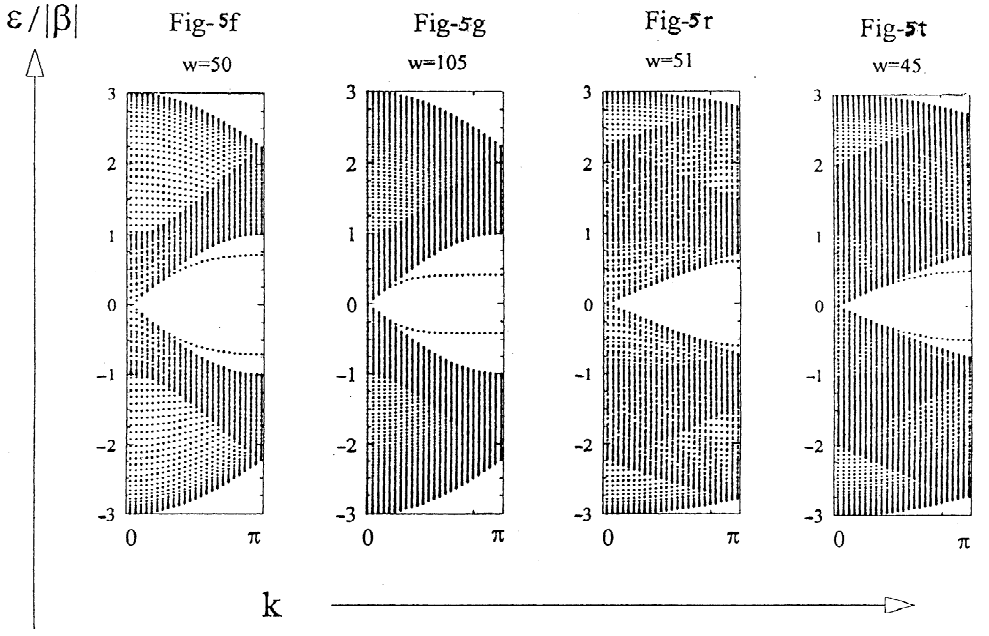

Fig. 11. Band eigenspectra (in units of $|\beta|$) displayed at a selection of 25k values uniformly spaced from $k = 0$ to $k = \pi$, for four width w strips each with different edge structures which give no nonbonding unpaired electrons (except for a touching of bands at $k = 0$). The structures for the four cases shown are (in order): edges as in Fig. 5(f) with $w = 40$; as in Fig. 5(g) with $w = 105$; as in Fig. 5(r) with $w = 23$; and as in Fig. 5(t) with $w = 25$.

more severe the greater the distance in the Brillouin zone of the near-non-bonding MO is from those for bulk-graphite MOs (in the 'shaded' regions). The MOs in the shaded regions have been found in the cases checked to be more or less uniformly spread across the strip. Moreover, the unpaired spin density seems to occur predominantly on

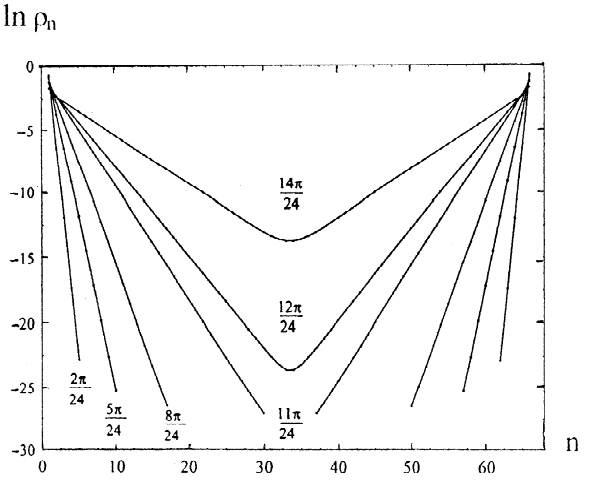

Fig. 12. Logarithms of frontier-orbital densities as a function of distance n from the edge of a width $w = 20$ graphitic strip with acenic edges (as in Fig. 4(a) or Fig. 6). The probability ρ_n represents binary sums of squares of MO coefficients at the nth starred and nth unstarred positions across the strip.

the same type (★ vs. ○) of sites in the resonance- and band-theoretic approaches. The results expounded here are also in agreement with several band-theoretic treatments elsewhere [38,21–37,39–48,56,81,82].

A fuller listing of comparative aspects for the edges of Fig. 5 are given in Table 1. The consequent RVB-theoretic predictions for the number $\#_u$ of unpaired electrons per unit cell of length are given in Table 1 for the two dozen edges indicated in Fig. 5. Table 1 also identifies the primitive translation (x,y) associated with each type of edge, where this (x,y) is identified as in the explanation surrounding Eq. (4). Finally in Table 1 references dealing with the various cases from the band-theoretic viewpoint are indicated, with the parenthetic references indicating some partial theoretical treatment, short of the computations such as reported in Figs. 10 and 11.

Notably there is unanimous quantitative agreement between $\#_u$ (from our resonance theory) and the number $\#_{NBMO}$ of nonbonding electrons per unit cell of edge length (from the band-theoretic computations). That is, we find

$$\#_{NBMO} = \#_u \tag{6}$$

for all translationally symmetric edges considered, including not only the representative cases of Figs. 10 and 11, but in fact all others occurring in Table 1. Further it turns out (as indicated in Fig. 12) that there seems to be qualitative agreement as to the location of the considered

Table 1
Edges, their symmetries, and edge-localized unpaired electrons per unit cell of edge

Structure in Fig. 5	Primitive translation (x,y)	Unpaired electrons, $\not\#_u$	Band theory references
(a)	(1,0)	1/3	[38,44,45,48]
(b)	(1,0)	2/3	[43]
(c)	(1,0)	1/3	[48,49]
(d)	(1,1)	0	[47,49]
(e)	(1,1)	1	[48]
(f)	(1,1)	0	[49], Here
(g)	(1,1)	0	[49], here
(h)	(2,0)	1/3	[48]
(i)	(2,0)	2/3	[49]
(j)	(2,0)	2/3	[49]
(k)	(2,0)	1/3	[48]
(l)	(2,0)	2/3	[48]
(m)	(2,1)	1/3	[47,48]
(n)	(2,1)	2/3	Here
(o)	(2,1)	2/3	Here
(p)	(2,1)	4/3	Here
(q)	(2,1)	2/3	Here
(r)	(2,2)	0	[49], Here
(s)	(2,2)	1	[49]
(t)	(3,0)	0	[49], Here
(u)	(3,0)	0	
(v)	(3,0)	0	
(w)	(3,1)	2/3	[47,49]

unpaired electrons. Here in Fig. 12 the densities ρ_n for an orbital of different indicated k from the exceptional band are plotted as a function of an average position n, where to suppress oscillations (between ★ and ○) ρ_n at a distance $n = d + 1/2$ from the edge is taken as the sum of the squares of orbital coefficients at the sites at distances d and $d + 1$ from the edge. The resonance theory evidently reveals an interesting pattern of behavior, giving ready insight into interesting chemicophysical characteristics of the various edge structures.

8. MO theoretic predictions for vacancy defects

These predictions might be sought to be checked via an MO theoretic approach. Of course with a local defect the translational symmetry of the graphite lattice is spoiled, so that ordinary band-theoretic computations are not directly applicable. Thus what one might do is simulate bulk graphite with 'suitable' large fragments, and delete a few sites from the center of the fragment to represent the defect. But to do this in practice it is crucial to understand which fragments might be 'suitable'—in particular if we are to look for (near) non-bonding MOs associated to the defect, it would be preferable to avoid other near non-bonding MOs, such as could arise with certain fragment edges or corners. But in fact because of the preceding sections we understand how to choose 'suitable' fragments. In particular an example of such a 'suitable' fragment would have edges and corners of the first (or second) types indicated in Fig. 13, and we have now performed computations for about a dozen antimolecules near the center of such a fragment, with $N = 684$ sites (before deleting the sites in the defect). Examination is made especially of the HOMO, and perhaps a few MOs nearby to $\epsilon = 0$ so as to ascertain their disposition in the defected fragment. The results of these examinations are indicated in Fig. 14, where there are plotted logarithms of mean MO densities as a function of the graphical distance n from the center of the central hexagon whereat the defect is placed. When there are several degenerate nonbonding MOs these plots use the average densities for these different orbitals, and when there are no nonbonding MOs the plot shows the density for the HOMO. At the top of each plot a depiction of the antimolecule **Я** is shown in bold, with a lighter hexagon showing the position of **Я** with respect to the central hexagon of the fragment. And yet further with each plot there is indicated the values of the orbital energies ϵ_i for the orbitals which are plotted, and in addition in parentheses are shown the energies ϵ_j for the next orbital away (from the perfectly nonbonding $\epsilon = 0$ value). Upon examination of the results in Fig. 14, one sees that the orbital densities for the orbitals anticipated to correspond to unpaired electrons, indeed generally have nonbonding energy. In fact this must be the case for the finite fragments used, since the Coulson–Rushbrooke theorem [60] applies, and with equal numbers of ★ and ○ sites before deletion of the defect, one sees that the unbalance of ★ and ○ in the defected fragment must match the unbalance of the deleted molecule R. The remaining orbitals (not so implied to be $\epsilon = 0$) are always

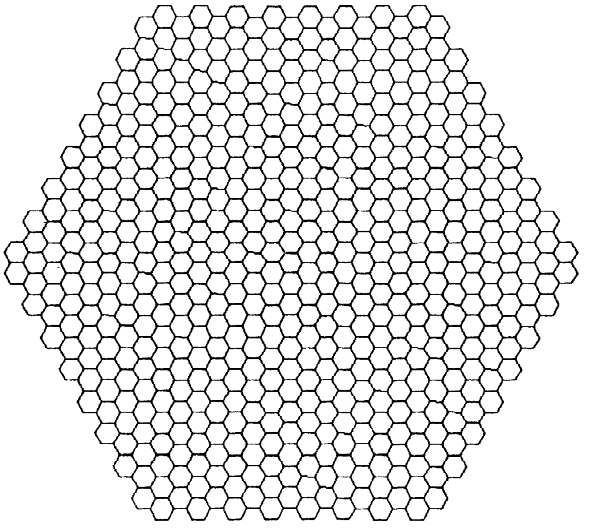

Fig. 13. Hexagonal-symmetry 1200-atom graphitic fragment, with edges (and corners) such as not to engender localized unpaired electrons at the periphery.

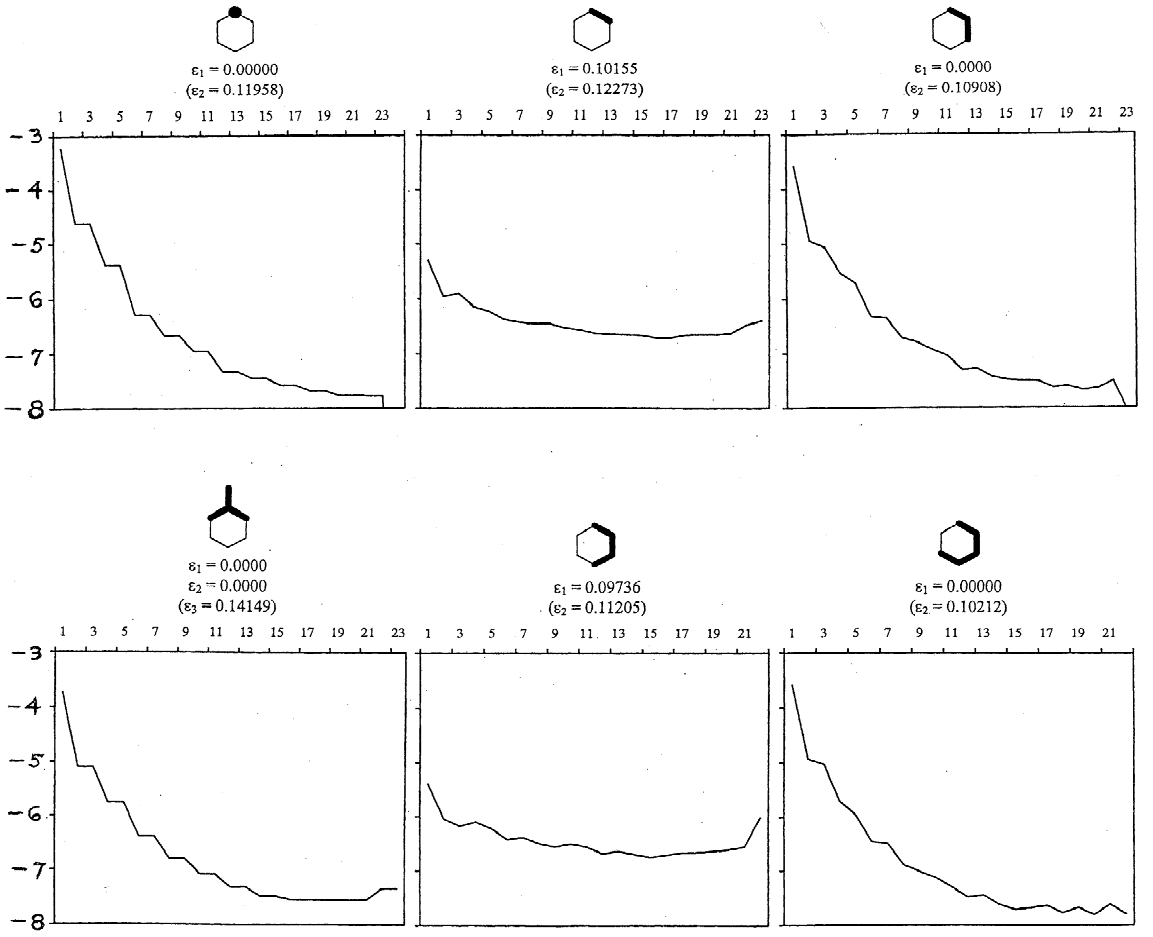

Fig. 14. Antimolecule electron densities for near-HOMOs as a function of the distance from the center of the graphitic fragment. The deleted sites of an antimolecule are identified by bold-face black substructures with otherwise only the central ring of the graphitic 1200-atom fragment being displayed. The values of the first few near-HOMOs are given with those nonparenthetic ones being included in the electron-density plot. Note that the two center plots (for antiethylene and antibutadiene) have a distribution which is much more nearly uniformily spread out than the other four antispecies, which are in fact predicted to have frontier (unpaired) electron density localized around the defect.

distinctly different in energy from $\epsilon = 0$, as perhaps could be surmised from the relatively large HOMO–LUMO gap in the undefected fragment. Moreover the nonbonding ($\epsilon = 0$) orbitals seem to be more localized in the region of the defect. In the cases (as antiethylene, antibutadiene and antibenzene) where no such defect-localized orbitals are expected, one sees that in fact the most nearly nonbonding MOs are in fact markedly more delocalized (i.e. more nearly constant, as gauged by the functional dependence of their average density on the distance from the center of the fragment). The decay of the $\epsilon = 0$ orbital densities away from the defect appears only roughly exponential, there evidently being some degree of interaction with the edges of the fragment, as does not seem so unreasonable since the present distances here are: first, somewhat smaller than the distances between strip edges which involved the nice exponential decay of Fig. 12. Still it appears that the number of such nonbonding defect-localized MOs generally exactly matches what is anticipated from our mean-field resonance theory—i.e. the number of such MOs for an antimolecule is just $|\#_{\bigstar} - \#_{\bigcirc}|$ for the corresponding molecule. Indeed such a result has been checked here and in [49] for several vacancy defects (identified as antimolecules Я) as indicated in Table 2.

Thus our mean-field resonance theory seems to correctly predict significant characteristics of these various antimolecules. Our plot of logarithmic density vs. distance for antimethyl deviates somewhat from linearity, presumably because of the edge in our finite-sized fragment. The resonance theory frequently predicts that the unpaired electrons lie predominantly on one type of site (★ or ○) and, though not shown in Fig. 14 because of the local

Table 2
Numbers of defect-localized unpaired electrons (at a defect Я obtained by deleting a molecule R from the graphite lattice)

R molecule (to be vacated)	# Я-localized unpaired e
Methyl	1
Ethylene	1
Allyl	1
Trimethylenemethyl	2
cis-Butadiene	0
trans-butadiene	0
cis,cis-Pentadienyl	1
cis,trans-Pentadienyl	1
trans,trans-Pentadienyl	1
Tetramethyleneethylene	0
2,4-Dimethylenepentadienyl	3
Benzene	0
Benzyl	1
1,3,5-Trimethylenebenzene	3

averaging, the MO computations then generally find the defect localized nonbonding MOs on the same type of sites. Thus general agreement is obtained between our MO computations and the resonance-theoretic predictions.

9. MO theoretic predictions for pairs of vacancy defects

The MO-based computations of the preceding section readily extend to the treatment of pairs of vacancy defects. Though the present approach may be applied with two (or more) antimolecule defects at different distances, we here illustrate the ideas in application to a pair of antimethyls. We may interpret what is going on in a picturesque manner. Evidently each antimethyl when alone gives rise to a nonbonding defect-localized MO, and when there is a pair of antimethyls we may imagine these two provisionally nonbonding MOs (say ϕ and ϕ') localized to different antimethyls (Я and Я′) as being only 0-order approximations, which may strongly interact with one another since they are degenerate (in 0-order). As it turns out this interaction (between ϕ and ϕ') is dramatically different depending on whether the two antimethyls (Я and Я′) are located at the same or different types of sites (★ or ○) in the graphitic network. And in fact this may be anticipated, since these 0-order nonbonding MOs (ϕ and ϕ') in addition to being defect-localized are typically localized on one type of site or the other. With this in mind, along with the recognition that the perturbation V simply involves a sum over (Hückel-like) near-neighbor electron-transfer interactions in the locality of each defect, one sees that the interaction $\langle\phi|V|\phi'\rangle$ should be most pronounced when ϕ and ϕ' are on different types of sites (★ or ○), whence the resultant admixtures of ϕ and ϕ' should no longer be nonbonding. The resultant energies for the interacting pair ϕ and ϕ' are then moved to values $\pm\langle\phi|V|\phi'\rangle$ in 1st order, which may be into the (quasi-) continuum of other (delocalized) graphitic levels, where they may further interact (in higher order) to become delocalized. One further sees that, as Я and Я′ separate ever farther, the matrix elements $\langle\phi|V|\phi'\rangle$ should become ever smaller (since ϕ is localized nearer Я while ϕ' is localized nearer Я′. Thus, granted that the single antimolecule MOs behave as anticipated in the preceding section, it is quite plausible that the nonbonding defect-localized MOs for each of two antimolecules interact to give the patterns anticipated, as explained here, and seen in Fig. 15. There for two antimethyls we plot mean orbital densities as a function of the distance n to the closest of two antimethyls for about a half-dozen different dispositions of the two antimethyls. For antimethyls in different hex-rings, we choose a graphitic fragment slightly modified from that of Fig. 13 to that of Fig. 16. Then the resultant densities for the HOMO as a function of distance n from the center are shown in Fig. 17. Notably from Figs. 15 and 17 we see agreement with the resonance-theoretic predictions. That is, the number of nonbonding defect-localized MOs matches the number of resonance-theoretically predicted unpaired electrons. In the 4th case (and perhaps the 5th case) of Fig. 17 we note that there seems to be a bonding–antibonding pair of localized electrons (such as is not considered in our present resonance-theoretic considerations), and indeed we have found this to occasionally happen with edges also.

10. Further local defects in graphite

A type of local defect involving different local connectivities is possible, differing from simple vacancies of one or more carbons. With different local connections there could conceivably be odd-cycles. For instance, out of the center of the 14-cycle of a pyrene ring the two central C-atoms could be deleted and replaced by a single CH group σ-bonded to two of the carbons, as in Fig. 18(a). But reservations arise, about both the simple resonance-theoretic and MO-theoretic approaches. The resonance-theoretic approach makes intimate use of starring and unstarring, which no longer occurs with odd-cycles. And for the Hückel-theoretic approach the presence of odd cycles generally leads [31] to a nonuniform distribution of charge (in the ground state), so that the interatomic Coulombic and electron–electron interactions absent from the simple Hückel model should be more important. Still in some sense the vast bulk of the material is bipartite (with consequent expected near uniformity of charge), indeed everywhere except in the defect region. So we might try to pursue a resonance-theoretic development as much as possible in concert with the sort of picture we

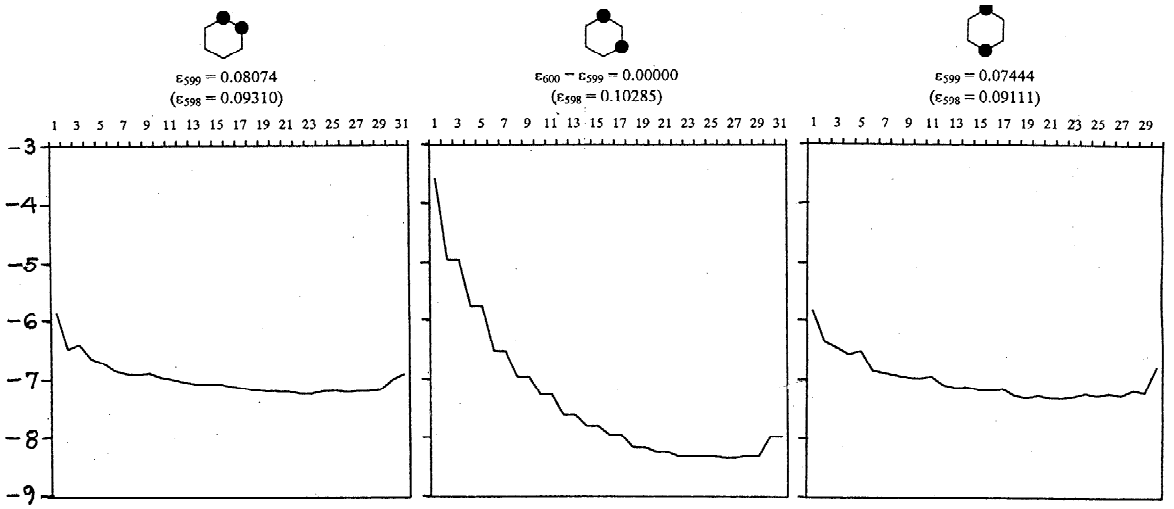

Fig. 15. Electron densities for near-HOMOs as a function of the distance from the center of the graphitic fragment (of Fig. 14) with two antimethyls in the central ring of the graphitic fragment. The deleted sites of an antimolecule are identified by black dots on those sites with only the central ring of the graphitic fragment being displayed. The values of the first few near-HOMOs are given with those nonparenthetic ones being included in the electron-density plot.

have for the bulk bipartite region, with provisional 0-order bond orders everywhere except on one of the central bonds, either of which if imagined to be deleted (or given a 0 bond order) leaves a bipartite structure, as indicated in Fig. 18(b), where there is some consequent additional spin pairing indicated by dotted lines. Within the context of simple MO theory, computations may be carried out on our large but finite fragment as in Fig. 16 but with a modification in the center as indicated in Fig. 18(a)—the result yielding a singly occupied HOMO with a density as a function of the graphical distance from the defect as indicated in Fig. 18(c). This evidently leaves a net one unpaired electron somewhere in the neighborhood of the defect. For the Hückel MO theoretic approach (with a five-membered ring in the center) the resultant singly occupied (nonbonding) MO appears to be defect-localized, and therefore agreement is attained with the prediction of the simple resonance theory. A few additional topological defects may be considered, with the resultant MO-theoretic computations indicated in Fig. 19. The first is a bipartite structure (closely related to the nonbipartite example of Fig. 18 and the first of the examples in Fig. 14), while the second and third structures here again are nonbipartite. Evidently gratifyingly general agreement between the resonance theoretic and MO theoretic predictions is still obtained.

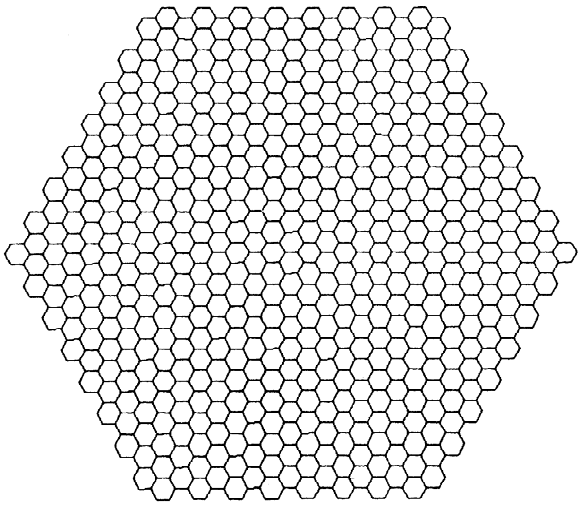

Fig. 16. C_{2v}-symmetry 1136-atom graphitic fragment, with edges (and corners) such as not to engender localized unpaired electrons. Here two hex-rings share an edge at the center.

11. Substitutional defects in graphite

It is natural to seek to extend the resonance theoretic arguments and simple MO theoretic computations to graphite with localized substitutional defects. For instance, a carbon atom might be substituted by an N^+, or by a B. In both these cases one has the same number of sites, though the first case gives no change in the number of π electrons, while the second case entails 1 fewer π electrons. Especially for edges, the presence of heteroatoms (e.g. involv-

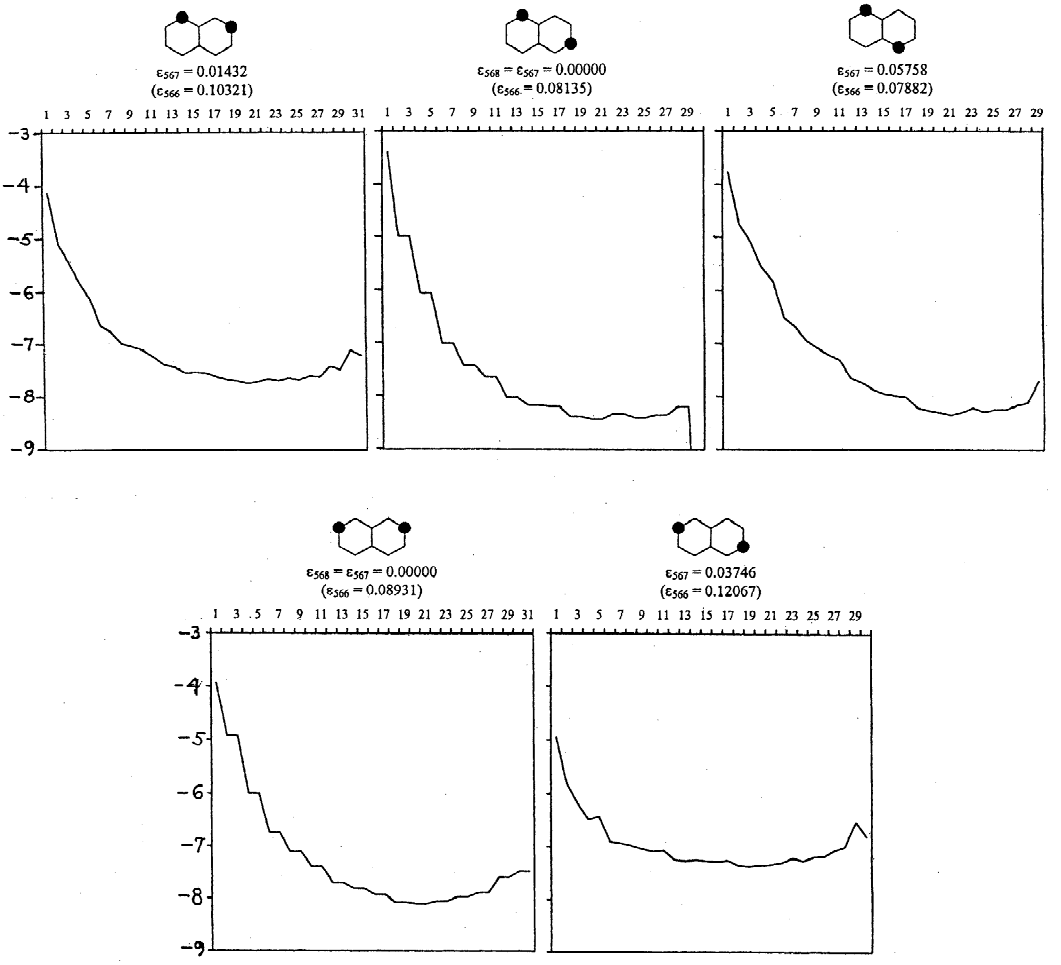

Fig. 17. Electron densities for near-HOMOs as a function of the distance from the center of the graphitic fragment (of Fig. 16) with two antimethyls in adjacent central rings of the graphitic fragment; notation as in Fig. 15.

ing O-atoms) has been suggested (e.g. in [20,83,84]) to be of relevance.

Thence one might investigate (at least as an initial step) the simplest extensions of the resonance- and MO theoretic approaches. With the assumption of resonance structures with fixed numbers of π electrons associated to each site it is still easy to make predictions. And within the framework of the Hückel π electron model with modified values for the associated heteroatom diagonal site energies (α_X for a heteroatom X) and perhaps also the associated electron transfer matrix elements (β_{CX} between C and X centers) it is possible to make computations comparable to those in the preceding two sections. However, it may be argued that the assumptions in this simple resonance theory as well as the simple MO model are more questionable for the case of heteroatoms. First, for resonance theory problems arise because it becomes more important to take explicit account of resonance structures with electrons transferred around between different centers; e.g. for the N^+ defect it may be important in the resonance-theoretic approach to take into account structures with an N center (with two π electrons) and a C^+ center someplace (presumably usually nearby). Second, for simple MO theory, questions arise as to the increased importance of the inclusion of more explicit Coulombic and electron–electron interactions, there being with heteroatoms more frequent nominally charged sites with electron pairs in close proximity. Despite these reservations one still might be tempted to compare resonance-theoretic predictions and the results of simple MO computations, and indeed we have done so for a handful of cases, to find frequent but not universal agreement between the two approaches. Because of these occasional presently unresolved disagreements we do not go further into this matter here, there evidently being additional refinement generally needed, for one or both of the two simple approaches we have been considering.

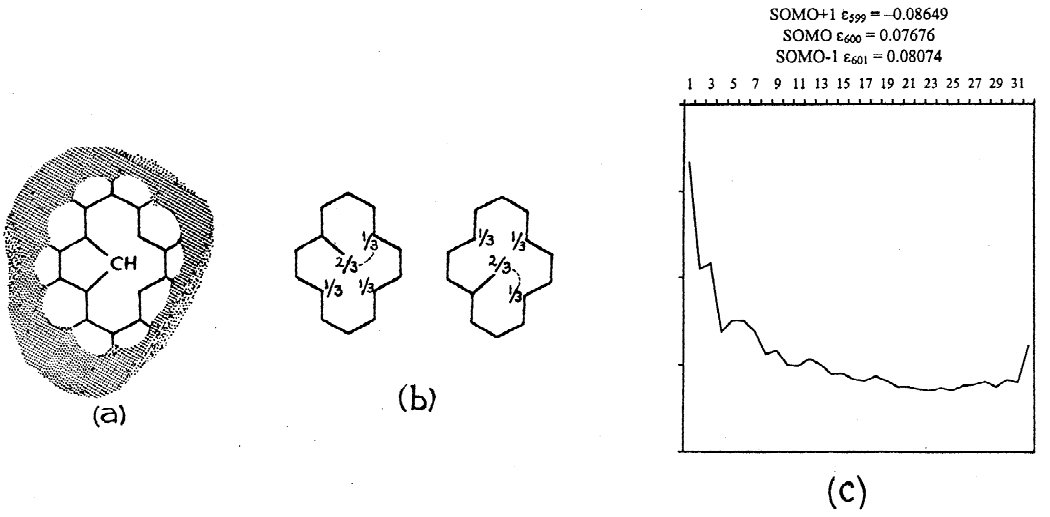

Fig. 18. Special central defect at the center of a graphitic fragment as in Fig. 16. The local defect structure is shown in (a), the manner of instituting a resonance-theoretic prediction is indicated in (b), and the MO theoretic HOMO-density as a function of distance from the center is shown in (c).

12. Discussion

The present ideas and results notably extend various earlier ideas, while also often simplifying the manner and generality of prediction. First, in Section 3 we indicated a wide range of well-documented agreement in working with ordinary benzenoid molecules. There are in addition a few more articles which address behaviors at edges or site vacancies in graphite, and provide some consistency with the picture developed here.

First, there has been some such work on site vacancies. For the case of a single-site defect considered by Coulson et al [50,51] solid evidence is found from both our qualitative resonance theory and quantitative MO theory that there is a single defect-localized unpaired π electron, though Coulson et al. did not look for evidence of this. But in this work of Coulson et al. [50,51] using finite fragments of the graphite lattice, the effect was complicated by other aspects: the poor choice for the type of edges on the fragments (such as we now understand engender their own

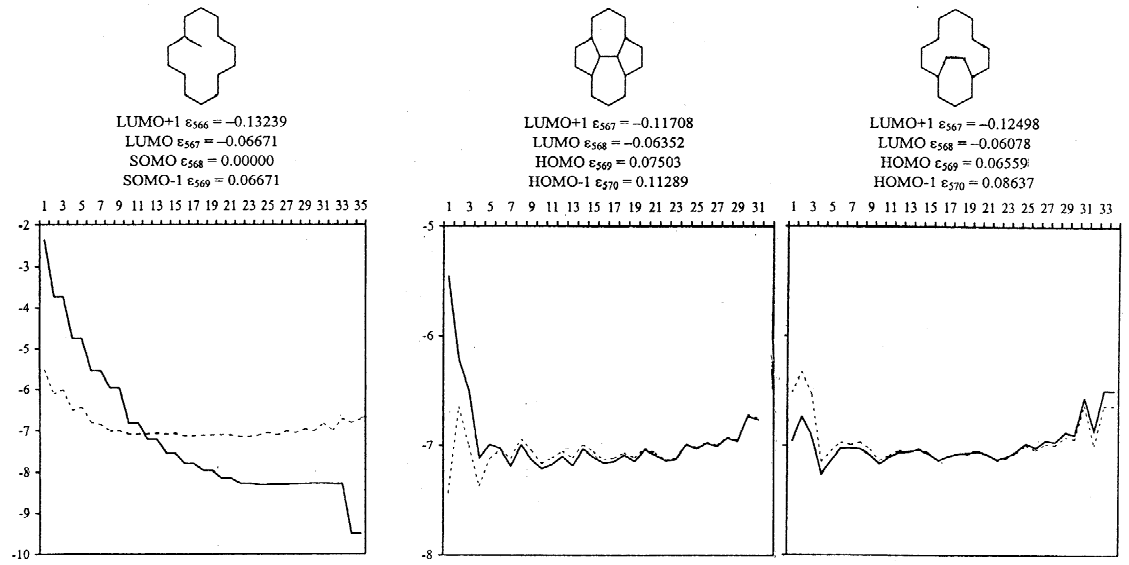

Fig. 19. HOMO densities for a few additional defects. The same sort of notational conventions as in Figs. 14,15 and 17 is used.

nonbonding MOs); the poor choice of 'shape' of fragment (such as to lead to an imbalance of starred and unstarred sites, and associated nonbonding MOs); and the relatively small size of the fragments (because of the more limited computer facilities then available). There is more recent theoretical work on the single-site defect [52–56], also by the MO approach, though most of these [53–55] seem not to consider the possibility of having (unpaired) spin density in the region of the defect, though they do find (in agreement with our picture) a local enhancement of charge density associated to near-nonbonding MOs in the region of the defect. Dietz et al. [52,56] suggest qualitatively in schematic diagrams that there is unpaired electron density near the vacancy, and especially in [56] they go on to treat quite large graphitic fragments, with a suitable noninterfering edge. But their focus seems to be on the energy cost of introducing the site vacancy. They also similarly treat the two-site vacancy. Their observations that their large one- and two-site vacated large molecules have overall spin doublet and singlet ground states is consistent with our result, though as we have emphasized in Section 3 there is much evidence that our scheme predicts correct overall spin multiplicity for quite general benzenoid molecules. Again the approach of the present paper treats more general defects particularly with multisite vacancies, with the vacancies either mutually adjoined or separated—and a general predictive result concerning defect-localized unpaired spins is obtained (in terms of an 'antimolecule' picture). Finally, there is explicit scanning-tunneling-microscopic (STM) observation [85–88] of single-site vacancy defects (and two-site defects in [88]), though the experimental documentation of any spin density around such defects is not yet attained. But in this experimental work there is observed an enhanced degree of electron density seen by the STM, and this is interpreted [53–55,85–88] to be due to additional density of near-nonbonding MOs (such as is in agreement with our picture). Further, larger multisite local defects occur as a result of etch pits, and STM depictions of these now becoming available [89–91], with quite small vacancy defects of say a half-dozen or so sites are sometimes seen [92].

The present predictions concerning edges, and in particular the unpaired electrons at certain sorts of edges turn out to be supported in earlier work. First, there is the work of Ref. [39] indicating some unpaired electrons localized at the zig-zag edge (first in Fig. 4) while there are no unpaired electrons for the armchair edges of the first in Fig. 3. This earlier work, though resonance-theory-based followed a traditional more explicit consideration of resonance-theoretic valence structures and their enumeration, so that dealing with each different type of edge was viewed as a separate rather formidable computational problem, while the present mean-field approach of Section 2 is applied with much easier argumentation. One resonance-theoretic approach also early investigated by Stein and Brown [40,42] assumes complete nearest-neighbor spin-pairings which is to say that this in essence assumes a complete dominance of spin-pairing over a maximal degree of resonance—that is, in terms of the two competing tendencies (loc and res) identified in Section 2, the approach they used assumed the complete dominance of loc over res. As a result of their detailed computations, different bulk amounts of resonance energy for different large graphitic fragments are estimated. Though this dominance assumption works well for small molecules (e.g. as in the work of Herndon [93,94] or of Randić [95,96]), one can expect that for large fragments this also misses the possibility of unpairing of electrons near edges. Still the resonance-theoretic work of Stein and Brown [40,42] may be seen to support our views in that the bulk graphitic resonance energies they compute under this restrictive assumption give higher values for the case of the zig-zag edge than for the armchair edge. That is, the values found by Stein and Brown are such that if unpairing were allowed this would occur with the zig-zag edge so as to enhance the bulk resonance energy and thereby bring the result more into coincidence with that for the armchair case. Further Stein and Brown's work [41,42] with the MO method on large graphitic fragments supports our case for edge-localized unpaired electrons in the case of the zig-zag edge, while again their results lead to the absence of unpaired spin density at the armchair edge. But rather than phrasing their results in terms of spin density based upon consideration of a uHF solution of something beyond a simple Hückel model (e.g. a PPP or Hubbard model), they point out the occurrence of (nearly) nonbonding edge-localized Hückel MOs, such as with additional (uHF-related) consideration lead to the conclusions concerning spin density. But a quantitative estimate of the number of unpaired electrons per unit cell of edge from Stein and Brown's MO work [41,42] is difficult because of the interference introduced by the corners they use in their finite-fragment approach. That is, MOs which are largely edge-localized for different edges on different sides of a corner are of course of similar energy and turn out to interact with one another so as to be shifted somewhat away from being nonbonding, which in turn tends to quench to some extent the spin density on adjacent different edges. The effects of the corners are considered in more detail from our point of view elsewhere [49]. Two other types of edges considered by Stein and Brown [40–42] both via their full-pairing resonance theory and by simple MO theory are similarly in agreement with our present picture, with the more extensive MO results for these edges being described elsewhere [48,49]. As already discussed (and illustrated) in Section 7 there now is quite good agreement of MO-based approaches for unpaired spin density at (certain) graphitic edges, in several works [43–48]. In [48] and [49] about two dozen different edges are treated via simple MO theory, and full agreement with the

resonance theory (as to the number of unpaired spins per unit length of edge) is found. Finally, Giunta and Kelty [97] report the observation via STM of both armchair and zig-zag types of edges, with the zig-zag ones occurring much less frequently perhaps because they might be less stable (as predicted via our resonance theory). These authors report extended Hückel computations on these two types of edges, these results further supporting our picture of edge-dependent patterns of unpaired spin density.

13. Conclusions

Simple structural rules governing the occurrence of free valences (or of locally unpaired spins) at graphitic defects or edges have been developed. These rules are somewhat intuitively derived (from chemically appealing resonance-theoretic ideas) in Section 2. The resultant rules near the end of Section 2 are emphasized to be quite simple to apply, as is illustrated for a variety of types of circumstances in following brief Sections 3–6. Numerous particular predictions for a variety of translationally symmetric edges are made in Table 1 (along with the associated Fig. 5) in Section 7. Predictions for the case of various vacancy defects are indicated in Table 2, in Section 8. Further in Sections 3–5, 7 and 8 some relevant general theorems are mentioned.

Overall our resonance-theoretic results find general support:

1. from the initially noted simple (yet presumably correct) classically plausible resonance-theoretic arguments (described in Section 2 here);
2. from more elaborated valence-bond-theoretic arguments (both theorematic and computational as briefly referenced in Section 3 here);
3. for studied cases (for graphitic strips and finite fragments) using MO-or band-theoretic arguments (as reported in [48,49] and in Sections 7–11 here); and
4. from some earlier (somewhat partial) theoretical results and experimental indications (as discussed in Sections 7 and 12)

Thus apparently the simple resonance-theoretic rules and the consequent predictions seem to hold exceptional promise for guidance as to the character of different possible edges and defects conceivable for graphitic materials. Presumably the edges or defects with higher concentrations of localized unpaired electrons would be reactive (as polyradicals) and under many preparatory conditions undergo additional reactions to quench this free valence.

Questions and associated qualifications concerning the present resonance-theoretic approach arise in seeking to extend it beyond benzenoid systems. We have found that this approach appears to extend successfully to nonbipartite (i.e. nonalternant) systems so long as the nonbipartiteness is confined within a local region, as briefly indicated in Section 10.

However, for the case of local heteroatom defects we have found limitations in one or both of the simple approaches. For structures with four cycles (or other $4n$ cycles) there is well-known reason to be cautious in applying resonance theory, because resonance around $4n$ cycles is not stabilizing (say as for the case of cyclobutadiene). Still there is notable interest in resonance-theoretic models for quite different four-cycle-containing systems, e.g. involving the square-planar lattice for the understanding of high-temperature superconduction [31–34], and also Pauling's theory of metals [98,99]. Hopefully the ideas developed here might still ultimately prove useful if suitably modified for such other systems, with nonbenzenoid rings or with heteroatoms. But despite these reservations the present ideas at least seem quite useful within the designated realm of applicability.

Acknowledgements

The authors thank a referee and Professor Radović for a number of helpful comments. Acknowledgment is made of support from the Welch Foundation of Houston, Texas.

References

[1] Kroto HW, Heath JR, O'Brien SC, Curl RF, Smalley RE. Nature 1985;318:162.
[2] Kratschmer W, Lamb LD, Fostiropoulos K, Huffman DR. Nature 1990;347:354.
[3] Iijima S. Nature 1991;354:333.
[4] Ebbesen TW, Ajayan PM. Nature 1992;358:220.
[5] Iijima S, Ichihashi T. Nature 1993;363:603.
[6] Smalley RE. Mater Sci Eng B 1993;19:1.
[7] Arayan PM, Iijima S. Nature 1993;361:33.
[8] Ebbesen TW. Physics Today (1996) 26.
[9] Hsu WK, Terrones M, Hare JP, Terrones H, Kroto HW, Walton DRM. Chem Phys Lett 1996;262:161.
[10] Endo M, Iijima S, Dresselhaus MS, editors, Carbon Nanotubes, New York: Pergamon, 1996.
[11] Yakobson BI, Smalley RE. Am Sci 1997;85:324.
[12] Donnet JB. Carbon 1982;20:267.
[13] Lewis IC. Carbon 1982;20:519.
[14] Wigmans T, Hoogland A, Tromp P, Moulijn JA. Carbon 1983;21:13.
[15] Ayache J, Oberlin A, Inagaki M. Carbon 1990;28:337.
[16] Mose-Yacaman M, Terrones H, Rendon L, Dominguez JM. Carbon 1995;33:669.
[17] McClure JW, Hickman BB. Carbon 1982;20:373.
[18] Ishii C, Shindo N, Kaneko K. Chem Phys Lett 1995;242:196.

[19] Ishii C, Matsumura Y, Kaneko K. J Phys Chem 1995;99:5743.
[20] Urry G. Elementary Equilibrium Chemistry of Carbon. New York: Wiley Interscience, 1989.
[21] Bradburn M, Coulson CA, Rushbrooke GS. Proc Roy Soc Edinburgh A 1948;62:336.
[22] Coulson CA, Rushbrooke GS. Proc Roy Soc Edinburgh A 1948;62:350.
[23] Wallace PR. Phys Rev 1947;71:622.
[24] Pauling L, Wheland GW. J Chem Phys 1933;1:362.
[25] Wheland GW. The Theory of Resonance. New York: Wiley, 1944.
[26] Pauling L. The Nature of the Chemical Bond. Ithaca, NY: Cornell University Press, 1939.
[27] Pauling L. Proc Natl Acad Sci 1966;56:1646.
[28] Klein DJ, Schmalz TG, Hite GE, Metropoulos A, Seitz WA. Chem Phys Lett 1985;120:367.
[29] Hite GE, Metropoulos A, Klein DJ, Schmalz TG, Seitz WA. Theor Chim Acta 1986;69:369.
[30] Klein DJ, Zhu H-Y, Valenti R, Garcia-Bach MA. Intl J Quantum Chem 1997;65:421.
[31] Manousakis E. Rev Mod Phys 1991;63:1.
[32] Barnes T. Intl J Mod Phys C 1991;2:659.
[33] Senatore G, March NH. Rev Mod Phys 1994;66:445.
[34] Dagotto E. Rev Mod Phys 1994;66:763.
[35] Cyvin SJ, Gutman I. Kekule Structures in Benzenoid Hydrocarbons. Springer Verlag, 1988.
[36] Davison S, Steślicka M. Basic Theory of Surface States. Oxford: Clarendon Press, 1992.
[37] Hoffmann R. Rev Mod Phys 1988;60:601.
[38] Coulson CA, Baldocks GR. Disc Faraday Soc 1950;8:27.
[39] Seitz WA, Klein DJ, Schmalz TG, García-Bach MA. Chem Phys Lett 1986;115:139.
[40] Stein SE, Brown RL. Carbon 1985;23:105.
[41] Stein SE, Brown RL. J Am Chem Soc 1987;109:3721.
[42] Stein SE, Brown RL. In: Liebman J, Greenberg A, editors, Molecular Structure and Energetics, Vol. 2, New York: VCH, 1987, pp. 37–66.
[43] Klein DJ. Chem Phys Lett 1994;217:261.
[44] Fujita M, Wakabayashi K, Nakada K, Kusakabe K. J Phys Soc Japan 1996;65:1920.
[45] Wakabayashi K, Fujita M, Kusakabe K, Nakada K. Czech. J. Phys. S4 46 (1996) 1865.
[46] Nakada K, Fujita M, Wakabayashi K, Kusakabe K. Czech. J. Phys. S4 46 (1996) 2429.
[47] Nakada M, Fujita M, Dresselhaus G, Dresselhaus MS. Phys Rev B 1996;54:17954.
[48] Klein DJ, Bytautas L. J Phys Chem 1999;103:5196.
[49] Ivancuic O, Bytautas L, Klein DJ. J Chem Phys, submitted for publication.
[50] Coulson CA, Herraez MA, Leal M, Santos E, Senent S. Proc Royal Soc Lond A 1963;274:461.
[51] Coulson CA, Poole MD. Carbon 1964;3:275.
[52] Tyutyulkov N, Madjarova G, Dietz F, Müllen K. J Phys Chem B 1998;102:10183.
[53] Lee KH, Causa M, Park SS. J Phys Chem B 1998;102:6020.
[54] Hjort M, Stafström S. Phys Rev B 2000;61:14089.
[55] Lee KH, Causa M, Park SS, Lee C, Suh Y, Eun HM, Kim D. J Mol Struct (TheoChem) 2000;506:297.
[56] Dietz F, Tyutyulkov N, Karabunarliev S, Hristov J, Müllen K. Polycyclic Aromatic Comp 1999;13:241–60.
[57] Klein DJ. In: Lahti P, editor, Magnetic Properties of Organic Materials, New York: Marcel Dekker, 1999, pp. 41–59.
[58] Rumer G, Nachr. Ges. Wis. Gött., Math-Physik Klasse (1932) 337.
[59] Rumer G, Teller E, Weyl H. Ges. Wis. Gött., Math-Physik Klasse (1932) 499.
[60] Coulson CA, Rushbrooke GS. Proc Camb Phil Soc 1940;36:193.
[61] Pauling L. J Chem Phys 1933;1:280.
[62] Simonetti M, Gianinetti E, Vandoni I. J Chem Phys 1968;48:1579.
[63] Pauncz R. Spin Eigenfunctions. New York: Plenum Press, 1979.
[64] Lieb EH, Mattis DC. J Math Phys 1962;3:749.
[65] Klein DJ, Nelin CJ, Alexander SA, Matsen FA. J Chem Phys 1982;77:3101.
[66] Parts 7-5 and 7-6 of the 1960 third edition of Ref. [26].
[67] Ham NS, Ruedenberg K. J Chem Phys 1959;29:1215.
[68] Lieb EH. Phys Rev Lett 1989;62:1201.
[69] Klein DJ, Alexander SA, Randić M. Mol Cryst Liq Cryst 1989;176:109.
[70] Cheranovski VO. Teor Eksp Khim 1980;16:147.
[71] Klein DJ, Alexander SA. In: King B, Rouvray DH, editors, Graph Theory and Topology in Chemistry, Amsterdam: Elsevier, 1987, pp. 404–19.
[72] Borden WT. J Am Chem Soc 1975;97:5968.
[73] Borden WT, Davidson ER. J Am Chem Soc 1977;99:4587.
[74] Borden WT, Davidson ER, Hart P. J Am Chem Soc 1978;100:388.
[75] Borden WT, Davidson ER, Feller D. J Am Chem Soc 1981;103:5725.
[76] Borden WT, Davidson ER. Acc Chem Res 1981;14:16.
[77] Chein JCW. Polyacetylene. New York: Academic Press, 1984.
[78] Chance RR, Boudreaux DS, Eckhardt H, Elsenbaumer RL, Frommer JE, Bredas JL, Silbey R. In: Ladik J et al., editor, Quantum Chemistry of Polymers—Solid State Aspects, D. Reidel, 1984, pp. 221–48.
[79] Klein DJ, Hite GE, Seitz WA, Schmalz TG. Theor Chim Acta 1986;69:409.
[80] Klein DJ, Schmalz TG, Seitz WA, Hite GE. Intl J Quantum Chem 1986;S19:707.
[81] Tyutyulkov NN, Madjarova G, Dietz F, Müllen K. Intl J Quantum Chem 1998;66:425.
[82] Bulusheva LG, Okotrub AV, Romanov DA, Tomanek D. Phys Low-Dim Struct 1998;3/4:107.
[83] Thomas JM. Carbon 1969;7:359.
[84] Pradhan BK, Sandle NK. Carbon 1999;37:1323.
[85] Rong ZY. Phys Rev B 1994;50:1839.
[86] Hahn JR, Kang H, Song S, Jeon IC. Phys Rev B 1996;53:R1725.
[87] Atamny F, Spillecke O, Schlögl R. Phys Chem-Chem Phys 1999;1:4113.
[88] Lee SM, Lee YH, Hwang YG, Hahn JR, Kang H. Phys Rev Lett 1999;82:217.
[89] Chang H, Bard AJ. J Am Chem Soc 1991;113:5588.
[90] Tracz A, Kalachev AA, Wegner G, Rabe JP. Langmuir 1995;11:2840.
[91] Manivannan A, Chirila M, Giles NC, Seehra MS. Carbon 1999;37:1741.
[92] Bourelle E, Konno H, Inagaki M. Carbon 1999;37:2041.

[93] Herndon WC. J Am Chem Soc 1973;95:2404.
[94] Herndon WC. Thermochim Acta 1974;8:225.
[95] Randić M. Tetrahedron 1977;33:1905.
[96] Randić M. J Am Chem Soc 1977;99:444.
[97] Giunta PL, Kelty SP. J Chem Phys 2001;114:1807.
[98] Pauling L. J Sol St Chem 1984;54:297.
[99] Kamb B, Pauling L. Proc Natl Acad Sci USA 1985;82:8284.